SUPPORTING INFORMATION FOR:

The Structure of Sodium Silicate Glass from Neutron Diffraction and Modelling of Oxygen-Oxygen Correlations

Alex C. Hannon[1], *Shuchi Vaishnav*[2,a], *Oliver L. G. Alderman*[1], *Paul A. Bingham*[2]

[1]ISIS Facility, Rutherford Appleton Laboratory, Chilton, Didcot, Oxon OX11 0QX, U.K.

[2]Materials and Engineering Research Institute, College of Business, Technology and Engineering, Sheffield Hallam University, Sheffield S1 1WB, U.K.

[a]Current address: Department of Materials Science and Engineering, Sir Robert Hadfield Building, Mappin Street, Sheffield S1 3JD, U.K.

S1. Na_2SiO_3 – determination of thermal width for Na-O bonds

S1.1. Experimental

A powder crystal sample of Na_2SiO_3 was obtained by conventional melting and natural cooling of a $50Na_2O{\cdot}50SiO_2$ glass. To prepare the composition, analytical grade Na_2CO_3 and pure SiO_2 (Alfa Aesar) were selected and weighed on a calibrated balance as per batch calculations. The batch ingredients were mixed homogenously and melted in a Pt-ZGS crucible with a Pt lid within an electric furnace at 1200^{o}C for 3 hours. The melt was poured on a clean stainless steel metal plate and allowed to cool to room temperature naturally. Due to the high concentration of Na_2O the melt crystallised during cooling.

Prior to the neutron diffraction measurement, the crystallinity of the sample was checked using Raman spectroscopy and X-ray diffraction. A Thermo Scientific DXRTM 2 Raman spectrometer installed with a laser of wavelength 532 nm and 10 mW power was used for the Raman scattering measurement. The laser beam was focused on the sample via a 50× lens. The grating was set to 900 lines/mm providing an estimated resolution between 5.5 - 8.3 cm^{-1} and spot size of 2.1 μm. Prior to the measurement, the spectrometer was calibrated with a certified polystyrene film. The scan was repeated 20 times within the frequency range of 100 - 2000 cm^{-1} and co-added to generate the final spectrum. The X-ray diffraction measurement was performed using a PANalytical Empyrean diffractometer, equipped with a silver anode X-ray tube. The finely

powdered sample was placed inside a 1 mm diameter silica glass capillary tube, sealed with beeswax. The X-ray diffraction pattern was measured for Bragg angles from 3.05º to 145.83º, with a step size of 0.1º. The Raman spectrum and the X-ray diffraction pattern of the Na_2SiO_3 sample are shown in Figures S1 and S2 respectively.

FIGURE S1 The Raman spectrum of the Na_2SiO_3 sample.

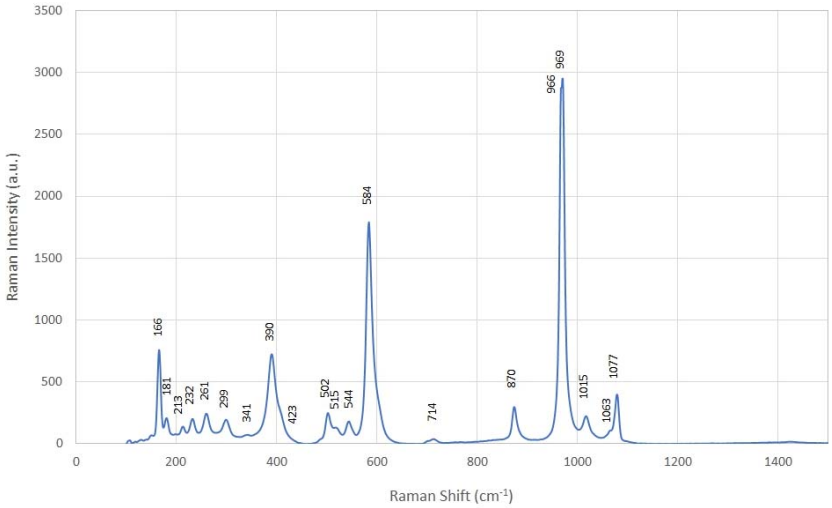

FIGURE S2 The X-ray diffraction pattern of the Na_2SiO_3 sample, after direct subtraction of the pattern for an empty capillary.

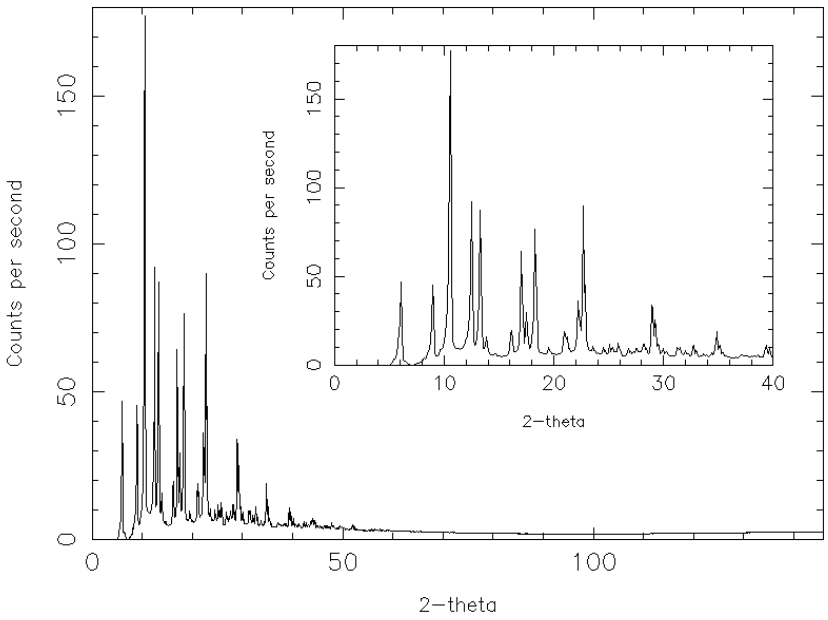

The measured Raman spectrum of the Na_2SiO_3 sample (Figure S1) is almost identical to that reported previously for sodium metasilicate by Richet and Mysen.[1] The Raman bands in the high frequency range 800-1200 cm^{-1} are due to Si-O stretching modes in the Q_n units. Crystalline

Na_2SiO_3 only contains Q_2 units,[2] whereas a glass phase normally has more than one Q_n species.[3] Thus a sample that contained a significant amount of glassy material would show broad Raman bands in the high frequency region, due to Q_n speciation. No such broadening was observed, showing that the sample contains little or no glassy material. The measured X-ray diffraction pattern (Figure S2) is typical of that for a powder crystal sample, and there is no discernible slowly changing background, as would be observed if the sample had a glassy component.

The powder sample of Na_2SiO_3 was loaded in a cylindrical vanadium container of internal and external diameters 3.81 cm and 3.94 cm, respectively. Neutron diffraction measurements were made using the GEM diffractometer[4] at the ISIS Facility pulsed neutron source. Figure S3 shows the neutron diffraction pattern of the sample, together with a prediction of the neutron diffraction pattern of Na_2SiO_3.[2] Note that the *Q*-resolution and Debye-Waller factors of the prediction have not been refined, so that the predicted peak widths and variation in peak heights across the pattern are not exactly the same as for the measurement. The important point about the comparison between measurement and prediction is that they have the same peaks at the same d-spacings, showing that the sample is indeed crystalline Na_2SiO_3. Furthermore, there is no slowly varying background between the Bragg peaks, and hence there is no evidence for a significant amount of glassy material in the sample.

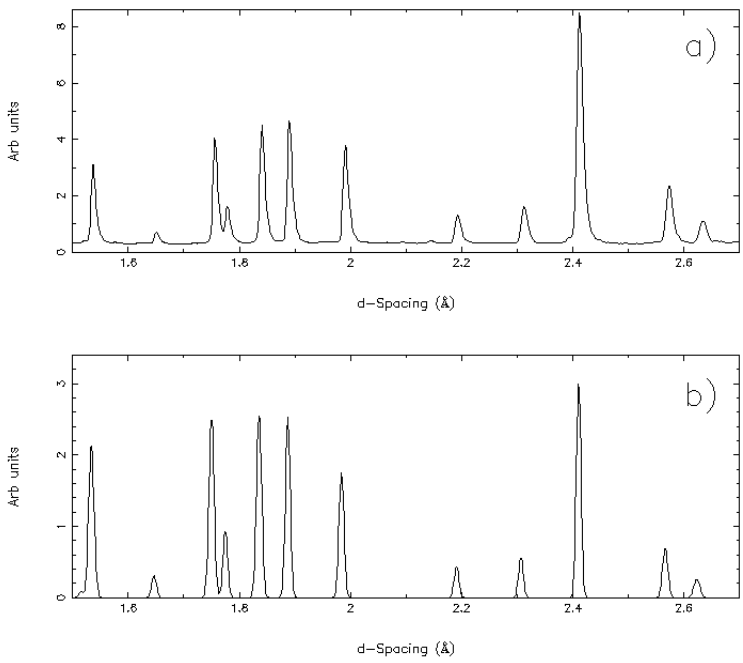

FIGURE S3 The neutron diffraction pattern of Na_2SiO_3. a) Measured by bank5 (~90º) of the GEM diffractometer. b) Predicted using CrystalMaker software[5-6] from a crystal structure report for Na_2SiO_3.[2]

The neutron diffraction results were corrected and analysed using ATLAS[7] and Gudrun[8] software, leading to the distinct scattering, $i(Q)$, shown in Figure S4a. The observed Bragg peaks are consistent with those calculated from a crystal structure report for Na_2SiO_3.[2] The experimental results for this sample are available on the ISIS Disordered Materials Database.[9]

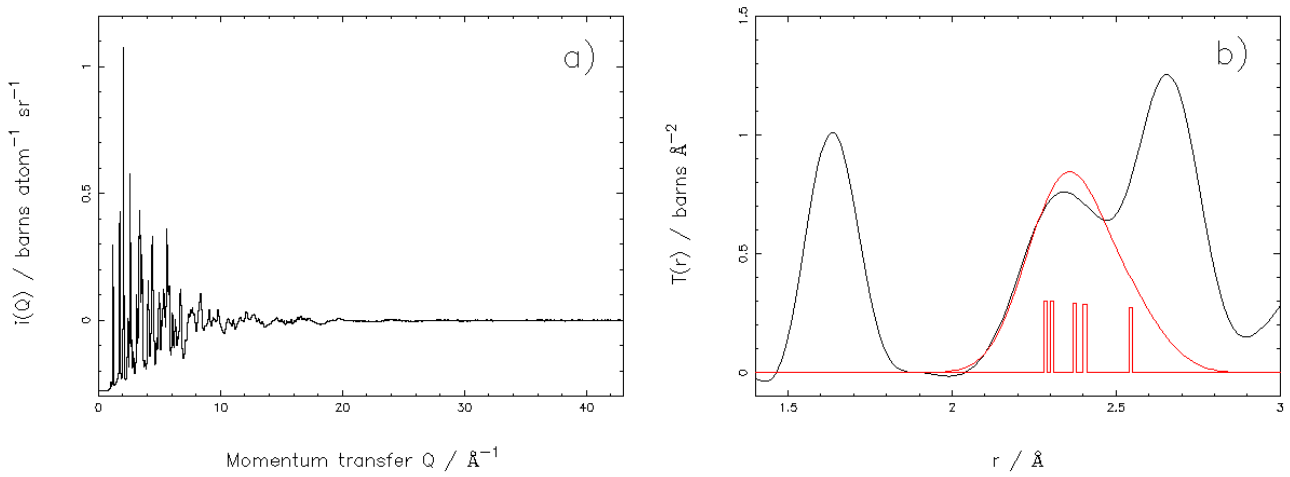

FIGURE S4 Neutron diffraction results for a powder crystal sample of Na_2SiO_3. a) The distinct scattering, $i(Q)$. b) The total correlation function, $T(r)$, together with a simulation of the Na-O contribution (red line – with broadening for real-space resolution and thermal motion; red histogram – without broadening, arbitrarily scaled).

S1.2. Determination of thermal width for Na-O bonds

The distinct scattering for Na_2SiO_3 was Fourier transformed using the Lorch modification function[10] with a maximum momentum transfer, Q_{max}, of 43 Å^{-1}, the same as for the glass correlation function shown in the main paper. The resultant total neutron correlation function, $T(r)$ is shown in Figure S4b (black line). The Na-O contribution to $T(r)$ was simulated from the structural information in the crystal structure report for Na_2SiO_3,[2] using *XTAL* software.[11-12] The red histogram in Figure S4b shows the Na-O contribution without broadening (arbitrarily scaled for convenience). The red line in Figure S4b shows the Na-O contribution after broadening for the effects of the experimental real-space resolution and thermal atomic motion.[13] The root mean square (RMS) variation in Na-O bond length, $\left\langle u^2_{\text{Na-O}} \right\rangle^{½}$, was adjusted to optimise the agreement with the experimental correlation function, and a value 0.095 Å was found to be optimal. For any value of $\left\langle u^2_{\text{Na-O}} \right\rangle^{½}$, the simulation and experimental result are not perfectly in agreement, which may be

evidence that a refinement of the crystal structure is required, but this is beyond the scope of the present work. Note that the value of $\left\langle u^2_{\text{Na-O}} \right\rangle^{½}$ obtained in this way represents thermal disorder only, and not static disorder, since the variation in the equilibrium values of the Na-O bond lengths is already taken into account in the structural information from the crystal structure report.[2] In contrast, the RMS variation in distance, $\left\langle u^2_{j-k} \right\rangle^{½}$, determined from fitting $T(r)$ for a glass usually represents both thermal and static disorder. The Na-O coordination number in crystalline Na_2SiO_3 is five; this value is closely similar to the value found for the sodium silicate glass, and hence the value of $\left\langle u^2_{\text{Na-O}} \right\rangle^{½}$ determined for this crystal can be expected to be closely similar to the value for the glass.

S2. Simulation of neutron correlation functions for sodium silicate crystal structures

S2.1. Thermal widths

The neutron correlation functions of sodium silicate crystals were simulated by *XTAL* software,[11-12] using the reported crystal structure. The simulated correlation functions were broadened for the effects of both real-space resolution and atomic motion, using respectively the Lorch modification function[13] (with Q_{max}=43 Å^{-1}, as for the measurement on the glass), and the thermal widths listed in Table S1. For longer distances, the values used for the thermal widths were calculated from the anisotropic thermal parameters reported for β-$Na_2Si_2O_5$.[14] At shorter interatomic distances, smaller values were used for the thermal widths to take into account the effect of correlated motion.[15-16]

TABLE S1 The thermal widths (RMS variation in interatomic distance), $\left\langle u_{j-k}^2 \right\rangle^{½}$, used to simulate the correlation functions of sodium silicate crystal structures. For most atom pairs a smaller value of $\left\langle u_{j-k}^2 \right\rangle^{½}$ was used for interatomic distances shorter than r_{cutoff}, and a larger value was used for longer interatomic distances.

Atom pair *j-k*	$\left\langle u_{j-k}^2 \right\rangle^{½}$ for short distances / Å	r_{cutoff} / Å	$\left\langle u_{j-k}^2 \right\rangle^{½}$ for long distances / Å
Si-Si	0.111		
Si-O	0.047	2.0	0.122
Si-Na	0.138		
O-O	0.091	3.0	0.135
Na-O	0.095	3.0	0.150
Na-Na	0.163		

S2.2. Simulations of the neutron correlation functions for β-$Na_2Si_2O_5$ and Na_2SiO_3

The simulated neutron correlation functions for β-$Na_2Si_2O_5$[14] and Na_2SiO_3[2] are shown in Figure S5.

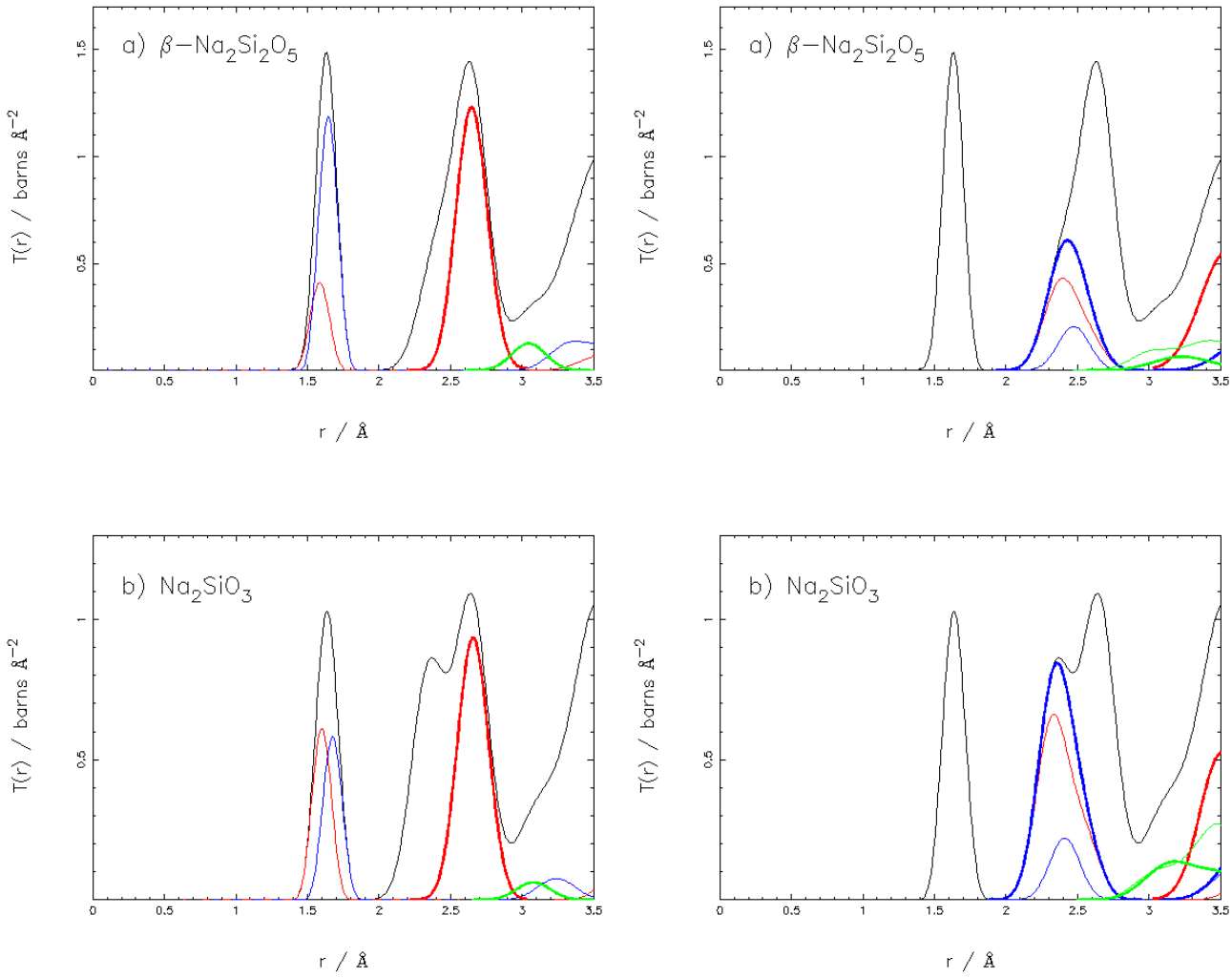

FIGURE S5 Simulation of the total neutron correlation function (thin black line), $T(r)$, for a) crystalline β-$Na_2Si_2O_5$,[14] and b) crystalline Na_2SiO_3.[2]

The left hand plots show the silicate partial contributions as follows: Si-NBO (thin red line), Si-BO (thin blue line), $(O\text{-}O)_{Si}$ (thick red line), and Si-Si (thick green line).

The right hand plots show the soda partial contributions as follows: Na-NBO (thin red line), Na-BO (thin blue line), total Na-O (thick blue line), $(O\text{-}O)_{Na}$ (thick red line), Na-Si (thin green line), and Na-Na (thick green line).

S3. Correlation function fitting software

A peak in a neutron (or X-ray) correlation function, $T(r)$, has a width larger than zero due to three effects:[13]

1. *Thermal motion of the atoms*. The thermal motion of the atoms gives rise to a broadening of a peak in the correlation function that is well represented by a Gaussian (see Equation (7)).
2. *Real-space resolution*. The correlation function is obtained by a Fourier sine transform of the distinct scattering, $i(Q)$, measured in reciprocal-space (where Q represents the momentum transfer for scattering). In principle, the integral of the Fourier transform should be performed over all Q-values from zero to infinity. In practice, the experimental data are truncated at some finite limit, Q_{max}, as represented by the modification function. This truncation leads to a broadening of the correlation function, and the consequent real-space resolution function is a Fourier cosine transform of the modification function [17].
3. *Static disorder*. This means that there is some variation in the distances between atom pairs of a particular type, with the result that there is a broadening of the corresponding peak in the correlation function. The difference between Si-NBO and Si-BO bond lengths (see Figure 7) can be regarded as static disorder amongst Si-O bonds.

The peaks in a correlation function may be fitted using appropriate software, such as the *pfit* suite of fitting programs.[18] The conventional approach is to fit each peak with a function that is a convolution of the real-space resolution function with a Gaussian. Because the real-space resolution function is not a Gaussian, there is loss of accuracy if a Gaussian is fitted,[19] and this is why dedicated fitting software should be used. The Gaussian represents principally the effect of thermal atomic motion. However, if there is static disorder that either involves a small range of distances compared to the other broadening effects, or is symmetric in form, then the fitted Gaussian can account for static disorder as well as thermal motion.

Three parameters are required to parameterise a (broadened Gaussian) peak in a correlation function. In the standard *pfit* program for fitting neutron correlation functions, a peak is parameterised by its position, $r_{j\text{-}k}$, its standard deviation, $\left\langle u_{j-k}^2 \right\rangle^{½}$, and its area, $A_{j\text{-}k}$. This area is proportional to $n_{j\text{-}k}/r_{j\text{-}k}$, where $n_{j\text{-}k}$ is the associated coordination number. However, it was found that using the standard approach, the areas on the two Na-O peaks (see Figure 5b) had large errors, because the two peaks are not well resolved. In this work, an alternative fitting approach was adopted, in which the third fitting parameter was coordination number, instead of area, and it was found that the errors on coordination number were much more reasonable, although the value for the overall Na-O coordination number was little changed. The sodium silicate glass measurement analysed in detail in this paper has previously been analysed as part of a study of the incorporation

of sulphate in silicate glasses.[20] In the previous report, the standard (area-based) fitting method was used, and hence there are differences in detail from the present report, which uses a coordination number-based fitting method.

S4. Correlation function for pure SiO_2 glass

The neutron diffraction pattern of a rod of high purity SiO_2 glass of diameter 8mm (Spectrosil WF, purchased from TSL Quadrant Ltd) was measured on the GEM diffractometer[4] at the ISIS Facility pulsed neutron source. The results were corrected and analysed using ATLAS[7] and Gudrun[8] software, leading to the neutron correlation function, $T_{SiO_2}(r)$, used for the application of the difference method shown in the main paper. The neutron diffraction data for SiO_2 glass are available from the ISIS Disordered Materials Database [9].

S5. Difference method Na-O fit

Two peaks were fitted to the apparent Na-O peak in the difference, $\Delta T(r)$, as shown in Figure 11, with the parameters given in Table S2.

Table S2 The parameters for the two-peak fit to the difference, $\Delta T(r)$, for the sodium silicate glass with 42.5 mol% Na_2O.

$r_{Na\text{-}O}$ / Å	$\langle u^2_{Na\text{-}O} \rangle^{½}$ / Å	$n_{Na\text{-}O}$
2.266(8)	0.091(4)	1.86(15)
2.422(5)	0.060(4)	1.09(15)

S6. Structural parameters of $Na_2Si_2O_5$ crystal polymorphs.

Table 2 of the main paper only includes the α and β forms of $Na_2Si_2O_5$, because crystallisation of glass shows that only these two polymorphs have any true range of thermodynamic stability.[21] However, several other forms of $Na_2Si_2O_5$ are known, and the structural parameters of all known forms are given in Table S3. Although there are some differences in the structural details between the different phases, they all obey the same rules, as discussed in sections 2.3 and 3.4. The same conclusions can be drawn from these parameters as are drawn from the parameters in Table 2.

Table S3 Structural parameters of $Na_2Si_2O_5$ crystal polymorphs. $\langle r_{Si\text{-}O}\rangle$ and $\langle r_{(O\text{-}O)Si}\rangle$ are respectively the mean Si-O bond length and the mean $(O\text{-}O)_{Si}$ distance, and $\langle \eta_{tet}\rangle$ is the mean tetrahedral distortion parameter (see Equation 13). $r_{Na\text{-}O,max}$ is the longest Na-O bond length, and the $n_{j\text{-}k}$ values are the various coordination numbers for sodium-oxygen interactions.

Compound	mol% Na_2O	$\langle r_{Si\text{-}O}\rangle$ / Å	$\langle r_{(O\text{-}O)Si}\rangle$ / Å	$\langle \eta_{tet}\rangle$	$r_{Na\text{-}O,max}$ / Å	$n_{Na\text{-}NBO}$	$n_{Na\text{-}BO}$	$n_{Na\text{-}O}$	$n_{NBO\text{-}Na}$	$n_{BO\text{-}Na}$	$n_{O\text{-}Na}$
α-$Na_2Si_2O_5$ [22]	33.33	1.6169	2.6409	0.99981	2.600	4	1	5	4	0.67	2
β-$Na_2Si_2O_5$ [14]	33.33	1.6243	2.6545	0.99922	2.588	4	1.5	5.5	4	1	2.2
γ-$Na_2Si_2O_5$ [23]	33.33	1.6206	2.6393	1.00271	3.055	3.21	2.21	5.42	3.21	1.47	2.17
δ-$Na_2Si_2O_5$ [24]	33.33	1.6193	2.6407	1.00138	2.572	4	1	5	4	0.67	2
ε-$Na_2Si_2O_5$ [25]	33.33	1.6283	2.6602	0.99957	2.865	4	2	6	4	1.33	2.4
κ-$Na_2Si_2O_5$ [26]	33.33	1.6203	2.6468	0.99967	2.910	4	1.5	5.5	4	1	2.2
HT-$Na_2Si_2O_5$ [23]	33.33	1.6113	2.6443	0.99504	3.134	4	3	7	4	2	2.8
C-$Na_2Si_2O_5$ [27]	33.33	1.6245	2.6543	0.99945	2.982	4	1.5	5.5	4	1	2.2

S7. References

1. Richet P, Mysen BO Andrault D. Melting and premelting of silicates: Raman spectroscopy and X-ray diffraction of Li_2SiO_3 and Na_2SiO_3. Phys Chem Min. 1996;23:157-172.
2. McDonald WS Cruickshank DWJ. A reinvestigation of the structure of sodium metasilicate, Na_2SiO_3. Acta Cryst. 1967;22:37-43.
3. Maekawa H, Maekawa T, Kawamura K Yokokawa T. The structural groups of alkali silicate glasses determined from ^{29}Si MAS-NMR. J Non-Cryst Solids. 1991;127:53-64.
4. Hannon AC. Results on disordered materials from the GEneral Materials diffractometer, GEM, at ISIS. Nucl Instrum Meth A. 2005;551:88-107.
5. Palmer DC. Visualization and analysis of crystal structures using CrystalMaker software. Z Kristallogr. 2015;230:559-572.
6. CrystalDiffract®: A powder diffraction program for Mac and Windows. Oxford: CrystalMaker Software Ltd, 2019 www.crystalmaker.com.
7. Hannon AC, Howells WS Soper AK. ATLAS: A suite of programs for the analysis of time-of-flight neutron diffraction data from liquid and amorphous samples. Inst Phys Conf Ser. 1990;107:193-211.
8. Soper AK, "GudrunN and GudrunX : Programs for correcting raw neutron and X-ray diffraction data to differential scattering cross section." In**.** Rutherford Appleton Laboratory Technical, 2011.
9. Hannon AC. Neutron diffraction database, http://www.alexhannon.co.uk/.
10. Lorch E. Neutron diffraction by germania, silica and radiation-damaged silica glasses. J Phys C. 1969;2:229-237.
11. Hannon AC, "XTAL: A program for calculating interatomic distances and coordination numbers for model structures." In *Rutherford Appleton Laboratory Report RAL-93-063***.** Rutherford Appleton Laboratory, 1993.
12. Hannon AC. XTAL structural modelling software, http://www.alexhannon.co.uk/.
13. Hannon AC. Neutron diffraction techniques for structural studies of glasses. In: Affatigato M, editor. Modern glass characterization**.** New York: Wiley, 2015; p. 158-240.
14. Pant AK. A reconsideration of the crystal structure of β-$Na_2Si_2O_5$. Acta Cryst B. 1968;24:1077-1083.
15. Jeong IK, Heffner RH, Graf MJ Billinge SJL. Lattice dynamics and correlated atomic motion from the atomic pair distribution function. Phys Rev B. 2003;67:104301.
16. Barney ER, Hannon AC Holland D. Short range order and dynamics in crystalline α-TeO_2 J Phys Chem C. 2012;116:3707-3718.
17. Johnson PAV, Wright AC Sinclair RN. Neutron scattering from vitreous silica II. Twin-axis diffraction experiments. J Non-Cryst Solids. 1983;58:109-130.
18. Hannon AC. PFIT correlation function fitting software, http://www.alexhannon.co.uk/.
19. Wright AC. Neutron and X-ray Amorphography. In: Simmons CJ and El-Bayoumi OH, editor. Experimental Techniques of Glass Science**.** Westerville: American Ceramic Society, 1993; p. 205-314.
20. Vaishnav S, Hannon AC, Barney ER Bingham PA. Neutron diffraction and Raman studies of the incorporation of sulfate in silicate glasses. J Phys Chem C. 2020;124:5409-5424.
21. Williamson J Glasser FP. Crystallisation of $Na_2O.2SiO_2$-SiO_2 glasses. Phys Chem Glasses. 1966;7:127-+.
22. Pant AK Cruickshank DWJ. The crystal structure of α-$Na_2Si_2O_5$. Acta Cryst B. 1968;24:13-19.
23. Kahlenberg V, Rakic S Weidenthaler C. Room- and high-temperature single crystal diffraction studies on γ-$Na_2Si_2O_5$: an interrupted framework with exclusively Q^3-units. Z Kristallogr. 2003;218:421-431.
24. Kahlenberg V, Dörsam G, Wendschuh-Josties M Fischer RX. The Crystal Structure of δ-$Na_2Si_2O_5$. J Solid State Chem. 1999;146:380-386.
25. Fleet ME Henderson GS. Epsilon sodium disilicate: A high-pressure layer structure [$Na_2Si_2O_5$]. J Solid State Chem. 1995;119:400-404.
26. Rakic S, Kahlenberg V Schmidt BC. Hydrothermal synthesis and structural characterization of κ-$Na_2Si_2O_5$ and $Na_{1.84}K_{0.16}Si_2O_5$. Solid State Sci. 2003;5:473-480.
27. Rakic S, Kahlenberg V, Weidenthaler C Zibrowius B. Structural characterization of high-pressure C-$Na_2Si_2O_5$ by single-crystal diffraction and ^{29}Si MAS NMR. Phys Chem Min. 2002;29:477-484.